EFFECTS OF FLOOR LOCATION ON RESPONSE OF COMPOSITE FUSELAGE FRAMES

Huey D. Carden and Lisa E. Jones
NASA Langley Research Center
Hampton, VA

Edwin L. Fasanella
Lockheed Engineering and Sciences Company
Hampton, VA

SUMMARY

Experimental and analytical results are presented which show the effect of floor placement on the structural response and strength of circular fuselage frames constructed of graphite-epoxy composite material. The research was conducted to study the behavior of conventionally designed advanced composite aircraft components. To achieve desired new designs which incorporate improved energy absorption capabilities requires an understanding of how these conventional designs behave under crash type loadings. Data are presented on the static behavior of the composite structure through photographs of the frame specimen, experimental strain distributions, and through analytical data from composite structural models. An understanding of this behavior can aid the dynamist in predicting the crash behavior of these structures and may assist the designer in achieving improved designs for energy absorption and crash behavior of future structures.

INTRODUCTION

The Landing and Impact Dynamics Branch of NASA Langley Research Center has been involved in crash dynamics research since the early 1970's. For the first 10 years, the emphasis of the research was on metal aircraft structures for both the General Aviation Crash Dynamics Program (R1-13) and the Controlled Impact Demonstration (CID) Program, a transport aircraft program which culminated in the controlled crash test of a Boeing 720 aircraft in 1984 (R14-16). Subsequent to the transport work, the emphasis has been on composite structures. Currently, efforts in crash dynamics research are being directed in three areas: (1) developing a data base for understanding the behavior, responses, failure mechanisms, and general loads associated with the composite material systems under crash type loadings; (2) analytical studies/development relative to composite structures; and (3) full-scale tests of metal and composite structures to verify performance of structural concepts.

Considerable research has been conducted into determining the energy absorption characteristics of composites (R17-20) which indicated that composite structures, if properly designed, can absorb more energy than comparable aluminum structures. Because of the brittle nature of the composites, however, attention must be given to designs which will take advantage of their powerful energy absorbing material properties while providing desired structural integrity when the composites are fabricated into aircraft structural elements and substructures. To achieve the desired new designs requires an understanding of how the more conventional designs behave under crash loadings.

The purpose of this paper is to present experimental and analytical data from a study of the effect of floor placement on the structural response and strength of conventionally designed circular fuselage frames constructed of graphite-epoxy composite material. Response of the composite fuselage frame structures for different floor locations is illustrated through photographs, experimental results, and through analytical data from finite element structural models. The determination of the effect of the floor location on the structural response of fuselage frames will aid in the understanding and prediction of full-scale subfloor or fuselage response to crash loading. Consequently, data from the present study are also compared to experimental

dynamic strain measurements on two previously tested composite subfloor structures (R21-22). Utilizing such data to gain an understanding of the fundamental behavior of subfloor structures may lead to improved designs for better energy absorption under crash loading conditions.

TEST SPECIMENS

I-, J-, C- and Z-cross sections are often used for fuselage frames in metal aircraft and have also been proposed for composite aircraft structures because of their structural efficiency. Several circular frames with these cross-sections (F1) were fabricated for testing. Earlier research with a Z cross-section circular frame (R23) indicated that failure of the anti-symmetric Z-frame without skin was initiated by a torsional instability. These out-of-plane rotations created complex boundary conditions and increased the difficulty of testing and analyzing the section. Consequently, a 3.5 inch wide skin material was added to the I-, J-, and C- frame concepts which increased the torsional stiffness of the cross-sections and limited out-of-plane rotations and deformations, as does the actual skin material in a fuselage structure. The skin, a $[\pm 45/0/90]_{2s}$ lay-up sixteen ply (.08 inches) thick, was cocured with the 6 foot diameter frames. Lay-up of the frame was $[\pm 45/\mp 45/90/0_3]_s$. Both the skin and the frame were fabricated with AS4/5208 graphite-epoxy material. Only the I-frame is used in the study reported in this paper.

TEST APPARATUS AND PROCEDURE

F2 shows a typical set-up of a composite fuselage I-frame in a 120 000-lbf loading machine prior to a quasi-static test. A steel I-beam was attached horizontally across the composite frame at the diameter position to simulate the floor. The horizontal floor positions were designated by the included angle measured between the ends of the floor attachments about the center of curvature of the frame. For example, the frame with the floor at the diameter is designated the 180° floor since the arc is 180° between the attachment points. A vertical compressive load was applied to the composite fuselage frame through the simulated floor beam and the lower platen of the load machine. Special clamps (See F2(d)) were used to bolt the I-beam to the composite frame and a 170° F melting point metal was poured into the small gap between the clamp and the frame to eliminate possible motion in the joint. As shown in F2(b) and 2(c), additional tests were conducted wherein the floor location was moved to produce 120°, and 90° arcs. In each test the specimen was loaded at a rate of 500 lbf/minute up to a maximum of 1000 lbf. Up to 64 channels of strain (for the 180° floor) as well as vertical load and vertical displacement were recorded at a rate of 8 sample/sec (initial test was 16 samples/sec) using a PC-based data acquisition system. Details of strain gage lay outs on the composite I-frame are shown in F3 and TI. A commercial software program was utilized to condition, convert data to engineering units, filter, and process the data for display.

ANALYSIS TOOLS

To gain an understanding of the physics of behavior, the experimental research of structures under crash loadings is generally accompanied by analytical prediction or correlation studies whenever feasible. Thus, various finite element codes which have capabilities for handling dynamic, large displacement, non-linear response problems of metal and composite structures were used as tools in the research efforts.

DYCAST Computer Code

The analytical results presented in this paper were generated with a nonlinear finite element computer code called DYCAST (DYnamic Crash Analysis of STructures (R24) developed by Grumman Aerospace Corporation with principal support from NASA and the FAA. The basic element library consists of (1) stringers or rod elements with axial stiffness only; (2) three-dimensional beam elements with 12 fixed cross-sectional shapes typical of aircraft structures with axial, two shear, torsional, and two bending stiffnesses; (3) isotropic and orthotropic membrane skin triangles with membrane stiffnesses; (4) isotropic plate bending triangles with membrane and out-of-plane bending stiffnesses; and (5) nonlinear translational or rotational spring elements that provide stiffness with user-specified force-displacement or moment-rotation tables (piece-wise linear). The spring element can be either elastic or dissipating. The

springs are useful to model crush behavior of components for which data are available and/or whose behavior may be too complex or time consuming to model otherwise. Curved composite beams, composite plate and curved shell elements were not available in the DYCAST element library at the time of this study.

In the present study two different analytical models, both with straight beam elements, were used for predicting response of the composite fuselage I-frame. One model designated as the compound beam was somewhat more detailed than the second simpler I-beam element model. F4 illustrates cross-sectional details of each of the two analytical model formulations.

Compound Beam Model.- Since the skin portion of the fuselage frame had a different lay-up and hence had a different stiffness from the I-frame, a compound beam approach was used to represent the frame in modeling the composite fuselage structure. In the compound beam model (See F4(a)), the I portion of the frame was modeled using a straight I-beam (ISEC) with appropriate material properties; whereas, the 0.08 inch thick skin was modeled with the solid rectangular beam (SREC) with appropriate but different material properties. The program allows these two different sections to be combined to act as a unit where specified geometry locates grid points, shear centers and centroid points at the appropriate location in the cross-section of the combination. A total of 78 elements (39 I-beam and 39 rectangular beam elements) were used in the model of the 180° fuselage frame. Symmetry about the ground contact point was used, thus only half of the 180° frame segment had to be discretized in the model. For the other floor positions, the model was reduced by the appropriate number of elements to represent the shorter frame segments.

I-Beam Model.- In the case of the I-beam model (See F4(b)), the combination of skin and I-frame were modeled with only I-beam elements. Since the skin lay-up provided less stiffness than the lay-up of the I-frame, the skin width was reduced by the ratio of the computed stiffnesses of the skin to the I-frame. As a result, the 3.5 inch skin width was reduced to approximately the same 2.5 inch width as the bottom flange of the I-frame itself. Thus, the resulting model consisted of straight ISEC elements wherein the bottom flange and skin were combined to be 0.16 inches in thickness with only the material properties of the I-frame being used in the model. Only half as many I-beam elements were needed as for a comparable compound beam model. The analytical results of the two different models are compared to each other and to the experimental data in the following section.

RESULTS AND DISCUSSION

F5-9 present results from studies with composite fuselage frames under static loadings for different floor locations. Analytical results are compared to the experimental behavior of the composite frame structure. The behavior of these standard frames with different floor locations under the same loading condition is considered as a first step in the design process of new frame structures for improving energy absorption and crash behavior.

Static experiments.- F5(a) presents a typical static strain distribution from tests of the composite I-frame used in the present study with a simulated floor fabricated from a steel I-beam located at the 180° floor position. Strain as a function of the circumferential position in degrees is plotted for the outer skin, the center of the web, and the inner flange of the I-frame under a load of 1000 lbf. It should be noted that the outer skin exhibits a distribution which resembles a "sea gull" shape. This shape occurs because of the maximum compressive strain is at the contact region of the bottom of the frame with the platen (0° position), and two tensile strain maximums occur at ± 60° from the contact region. Strain in the web and inner flange is reversed relative to the skin. Near the contact region the strain is tensile and is higher in magnitude than the compressive strain in the skin.

A comparison of the strain distributions in the outer skin of the composite I-frame for the 180°, the 120° and 90° floors are presented in F5(b). The strain distributions for the 120° and 90° floor positions are similar to the 180° floor results. The constraint of the floor for the 90° and 120° has compressed the "sea

gull" strain distribution shape into the shorter arc length , otherwise the general shape still has the maximum strain at the 0° contact region and the two maximums at symmetric ± positions. Additionally, for the given 1000 lbf load the magnitude of the strain in the flanges and skin (not shown) for each of the lower floor positions was less than the 180° floor . The strains are lower because the bending moments are decreased and the effective global structural stiffness is increased as the structural frame arc length is decreased for the lower floor positions.

Static analytical studies.- To analytically demonstrate the behavior of the frames under load, two DYCAST finite element models were constructed to analyze the frame behavior. The frame model was loaded at the top node and a simulated ground plane modeled by ground contact springs resisted the vertical movement of the frame during load application. Boundary conditions were imposed at the bottom node of the model to account for the symmetrical situation, thus only half the frame had to be modeled. The top node was initially constrained to allow only vertical displacement simulating the effect of a very stiff floor across the frame diameter. The static analytical load was increased linearly to 1000 lbf in 50 pound increments.

Evaluation of the analytical strain distribution on the frame for the 180° floor position shown in F6(a) indicates a number of important points which include: (a) maximum strains for the 1000 lbf load were at the 0° or ground contact location with two secondary maximums occurring at symmetric locations between 45°-55° from the bottom contact area; (b) the predicted outer skin strain distribution exhibits the same "sea gull" shape as measured in the experiment; and (c) similar inverted circumferential strain distributions were noted for the center of the web and for the inner flange of the frame as occurred in the experiment.

F6(b) presents a comparison of the experimental outer skin strain with the predicted distribution with the original clamped boundary and vertical force loading on the analytical model. As may be noted, initial model results are similar to the experimental distribution ; however, the position of the maximum strain at approximately ±45° is lower than the experimental maximum which occurs at approximately ±60°. As a consequence, the agreement between the experimental and analytical strain magnitudes is substantially different . Careful comparison of the experimental set-up and the analytical simulation was made. It was noted that experimental boundary attachments do not physically permit the load to be applied through the shear center of the composite I-frame. In the analytical models, however, the load was being applied through the shear center. Consequently, the model was altered to allow in-plane rotation at the loading point and a load with an off-set (load and moment) was applied at the top node point. The off-set distance was varied from 1 to 3 inches.

The effects of the boundary (pinned and clamped) and load application changes on the predicted strain distribution with the I-beam model are shown in F6(c). A comparison of the analytical cases indicates a substantial effect of the new load introduction and boundary change on the behavior patterns of the strain distribution. The major effect on the distribution is the shift of the upper maximum strain locations from ±45° to approximately ±60°, and to increase the magnitude of the strain throughout all circumferential locations. An analytical case was also conducted with the load applied through the shear center where there was no off-set and in-plane rotation was allowed at the load point. As shown in F6(c), allowing the rotational degree-of-freedom at the pinned end load point produced the largest effect in the analytical results. As previously noted, two analytical models were formulated in the study, the compound beam and the I-beam models. F6(d) presents a typical comparison of the predicted strain distributions with the two models (off-set = 3 inches) with the experimental outer skin distribution. Results of the two analytical models are essentially the same with some small differences in the magnitude of the strain at the maximum compressive and tensile strain locations. The I-beam model appears to agree better with the experimental results. Therefore, for ease of computations, the remainder of the analytical results presented in the paper are from the simpler I-beam analytical model.

Once the effect of the loading and boundary application was established, more comprehensive comparisons of the experimental and analytical results were made. For example, F7(a) to 7(c) present typical comparisons of the analytical distributions of strain with the experimental distributions for the 180°, the 120°, and the 90° floor positions, respectively. The agreement in the magnitudes of the analytical and

experimental strains and the shape of the distributions are excellent.

In addition to the circumferential strain distributions, comparisons were also made, as shown in F8, between the predicted radial strain which is measured through-the-section and the experimental data for the 180° floor. Strains on the inner flange, the center of the web, and the outer skin at three circumferential locations of 7.5°, 17.5°, and 37.5° are presented. It may be noted that the analytical and experimental radial distributions are in excellent agreement for all three circumferential positions.

Comparison of Frame Behavior with Subfloors

The determination of the effect of the floor location on the structural response of fuselage frames has aided in the understanding and predicting of full-scale subfloor or fuselage response to crash loading. For example, F9(a) shows two composite subfloor specimens, skeleton and skinned, (See R21-22) which were statically and dynamically tested. F9(b) shows a comparison of the normalized experimental dynamic strain distribution on the flange of the skeleton subfloor and the skin location corresponding to the flange position of the skinned composite subfloor specimens with the analytical I-frame strain of the present study. The results from the simple frame show a strong similarity to the response of the more complex subfloors structures. The structures share in common the generally circular or cylindrical shape, the vertical loading situations, and under vertical loads have strain (moment) distributions which have maximums at the point of loading and at approximately ±45° to ±60°, depending on boundary conditions, around the circumference from the ground contact point. Analytical results show the same distribution with maximums corresponding to the experimental locations. Failures of the subfloor structures were noted between these same 45° to 60° circumferential locations in the dynamic tests (See R21).

Lessons Relearned

Often efforts can be diverted to the wrong area when poor correlation is obtained in an initial comparison of experimental data with analytical predictions. Several important lessons, both experimentally and analytically, were relearned in the current studies which should be emphasized when analyzing and testing both composite and metal structures. The lessons are: (1) simple boundary conditions, such as fully clamped, are difficult or impossible to achieve in real structures, (2) systematic variations of the analytical boundary and load application should be examined carefully to assess the influence and effects on the correlation prior to any large scale changes of the analytical model or experiment; and (3) experimental and analytical personnel should collaborate closely in their efforts. Being reminded of such lessons can help dynamists gain a better understanding of what to expect from such structures in crash-loading situations, and can guide analysts to formulate adequate analytical models for predicting structural response under crash loadings. The latter task is a difficult one for composite structures as well as for metal structures.

CONCLUDING REMARKS AND OBSERVATIONS

Some unique structural behavior results from the research with composite aircraft fuselage frames have been presented and discussed and analytical results have been included to help explain the behavior noted. From the observations made in the present study, the following conclusions are made:

(1) The effects on the response of the composite frame from changing the floor position in the composite frame were: (a) to alter the magnitude of the strain (moment) but not the common, general "sea gull" shape of the distribution under vertical loading; (b) to constrain the general "sea gull" shaped strain distribution to occur in the frame segment below the floor attachment locations; and (c) to increase the effective global structural stiffness of the frame as arc length of the frame was decreased.

(2) Correct simulation of the experimental boundary/load application to the frame was critical in obtaining good correlation between the analytical and experimental results.

(3) Analytical finite element models of the frame predicted the circumferential and radial strain magnitudes and distribution.

(4) Correlation of normalized experimental strain distributions for floor structures and the composite I-frame indicated that the behavior of the simpler structures embodied the behavior of the more complex structural components.

(5) Knowledge of unique and predictable strain responses of composite fuselage frames will be used to achieve better future designs for energy management in a crash situation.

(6) Important lessons relearned in the present study were that (a) simple boundary conditions, such as fully clamped, are difficult or impossible to achieve in real structures, (b) systematic variations of the analytical boundary and load application should be examined carefully to assess the influence and effects on the correlation prior to any large scale changes of the analytical model; and (c) experimental and analytical personnel should collaborate closely in their efforts.

REFERENCES

1. Alfaro-Bou, Emilio; and Vaughan, Victor L., Jr.: Light Airplane Crash Tests at Impact Velocities of 13 and 27 m/sec. NASA TP 1042, November 1977.

2. Castle, Claude B.; and Alfaro-Bou, Emilio: Light Airplane Crash Tests at Three Flight-Path Angles. NASA TP 1210, June 1978.

3. Hayduk, Robert J.: Comparative Analysis of PA-31-350 Chieftain (N44LV) Accident and NASA Crash Test Data. NASA TM 80102, October 1979.

4. Castle, Claude B.; and Alfaro-Bou, Emilio: Light Airplane Crash Tests at Three Roll Angles. NASA TP 1477, October 1979.

5. Vaughan, Victor L., Jr.; and Alfaro-Bou, Emilio: Light Airplane Crash Tests at Three Pitch Angles. NASA TP 1481, November 1979.

6. Vaughan, Victor L., Jr.; and Hayduk, Robert J.: Crash Tests of Four Identical High-Wing Single-Engine Airplanes. NASA TP 1699, August 1980.

7. Carden, Huey D.; and Hayduk, Robert J.: Aircraft Subfloor Response to Crash Loadings. SAE Paper 810614, April 1981.

8. Williams, M. Susan; and Fasanella, Edwin L.: Crash Tests of Four Low-Wing Twin-Engine Airplanes with Truss-Reinforced Fuselage Structure. NASA TP 2070, September 1982.

9. Carden, Huey D.: Correlation and Assessment of Structural Airplane Crash Data with Flight Parameters at Impact. NASA TP 2083, November 1982.

10. Carden, Huey D.: Impulse Analysis of Airplane Crash Data with Consideration Given to Human Tolerance. SAE Paper 830748, April 1983.

11. Castle, Claude B.; and Alfaro-Bou, Emilio: Crash Tests of Three Identical Low-Wing Single-Engine Airplanes. NASA TP 2190, September 1983.

12. Thomson, Robert G.; Carden, Huey D.; and Hayduk, Robert J.: Survey of NASA Research on Crash Dynamics. NASA TP 2298, April 1984.

13. Carden, Huey D.: Full-Scale Crash Test Evaluation of Two Load-Limiting Subfloors for General Aviation Airframes. NASA TP 2380, December 1984.

14. Hayduk, Robert J.(Editor): Full-Scale Transport Controlled Impact Demonstration. NASA CP 2395, April 1985.

15. Fasanella, Edwin L.; Widmayer, E.; and Robinson, M. P.: Structural Analysis of the Controlled Impact Demonstration of a Jet Transport Airplane. AIAA Paper 86-0939-CP, May 1986.

16. Fasanella, Edwin L.; Alfaro-Bou, Emilio; and Hayduk, Robert J.: Impact Data from a Transport Aircraft During a Controlled Impact Demonstration. NASA TP 2589, September 1986.

17. Farley, Gary L.: Energy Absorption of Composite Materials. NASA TM 84638, AVRADCOM TR-83-B-2, 1983.

18. Bannerman, D.C.; and Kindervater, C.M.: Crashworthiness Investigation of Composite Aircraft Subfloor Beam Sections. IB 435-84/3(1984), Deutsche Forschungs-und Versuchasanstalt fur Luft- und Raumfarht, February 1984.

19. Cronkhite, J.D.; Chung, Y.T.; and Bark, L.W.: Crashworthy Composite Structures. ASAAVSCOM TR-87-D10, U.S. Army, December 1987. (Available from DTIC as AD B121 522.)

20. Jones, Lisa E.; and Carden, Huey D.: Evaluation of Energy Absorption of New Concepts of Aircraft Composite Subfloor Intersections. NASA TP 2951, November 1989.

21. Carden, Huey D.; and Robinson, Martha P.: Failure Behavior of Generic Metallic and Composite Aircraft Structural Components Under Crash Loads. NASA RP 1239, November 1990.

22. Boitnott, Richard L.; and Fasanella, Edwin L.: Impact Evaluation of Composite Floor Sections. SAE Paper 891018, General Aviation Aircraft Meeting and Exposition, Wichita, Kansas, April 1989.

23. Boitnott, Richard L.; Fasanella, Edwin L.; Calton, Lisa E.; and Carden, Huey D.: Impact Response of Composite Fuselage Frames. SAE Paper 871009, April 1987.

24. Pifko, A.B.; Winter, R.; and Ogilvie, P.L.: DYCAST - A Finite Element Program for the Crash Analysis of Structures. NASA CR 4040, January 1987.

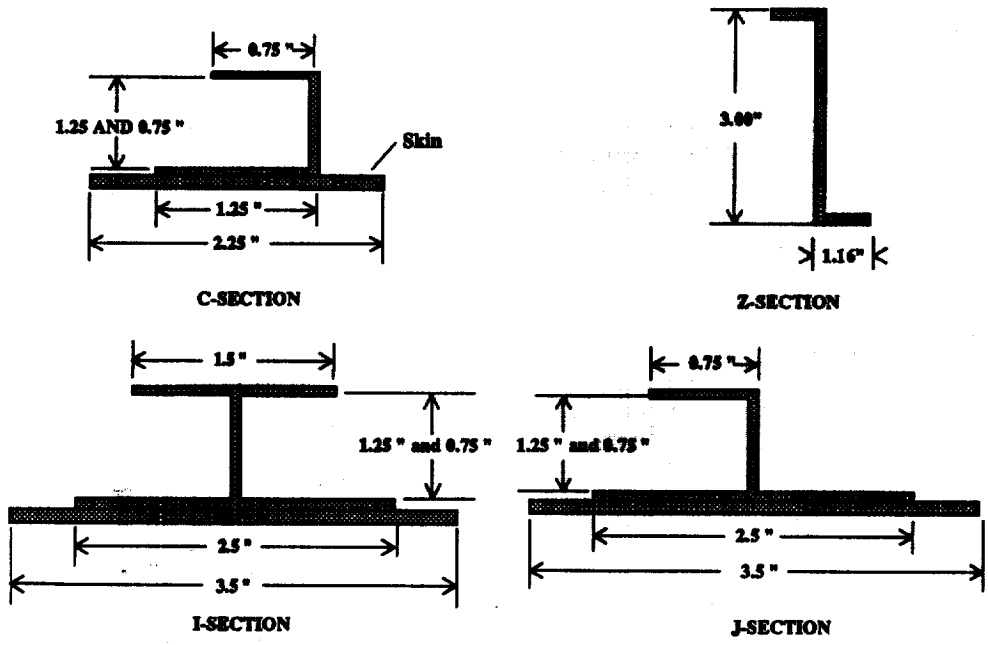

Figure 1.- Typical cross-sections of composite fuselage frame concepts.

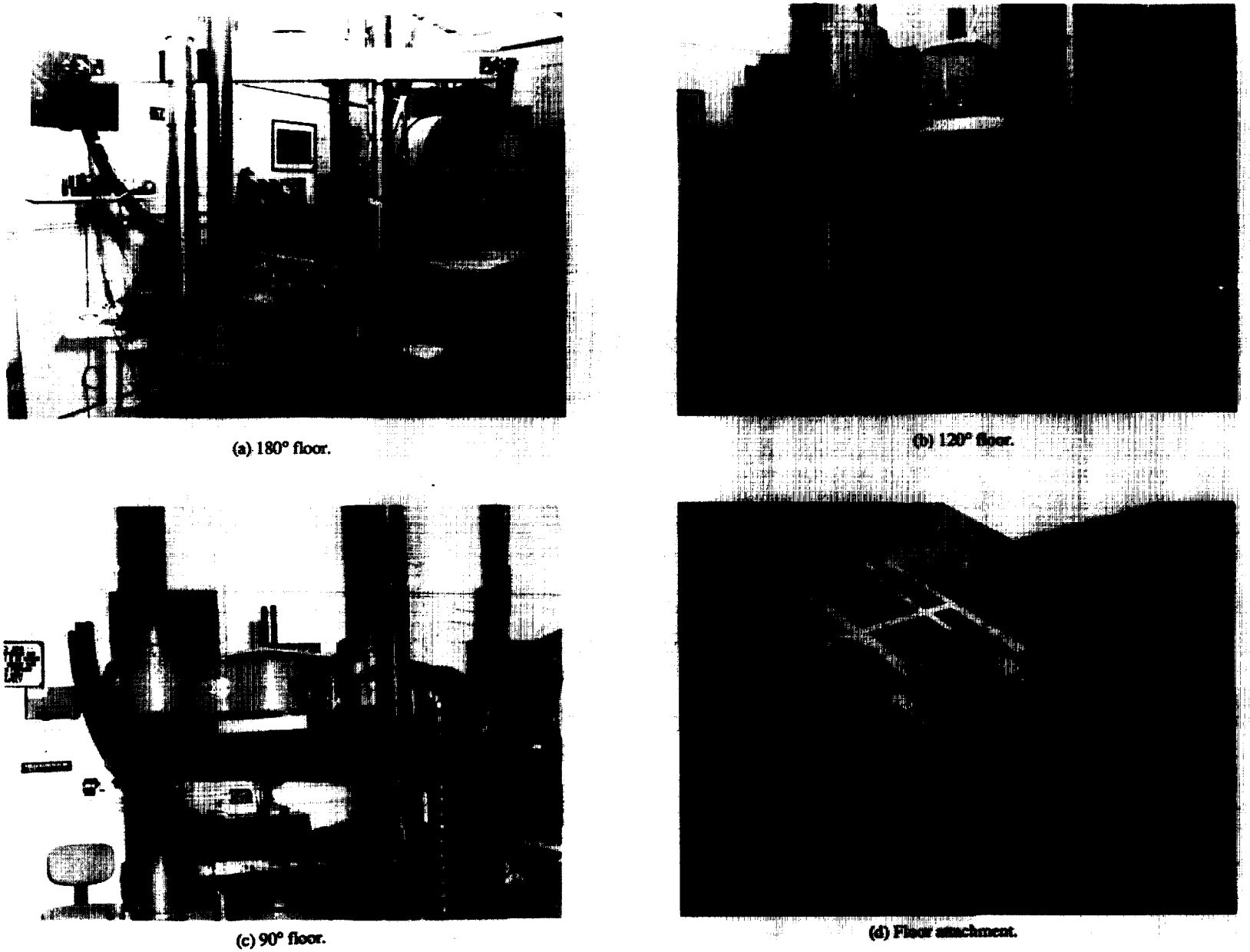

(a) 180° floor.

(b) 120° floor.

(c) 90° floor.

(d) Floor attachment.

Figure 2.- Typical experimental set-up of composite I-frame in static testing machine.

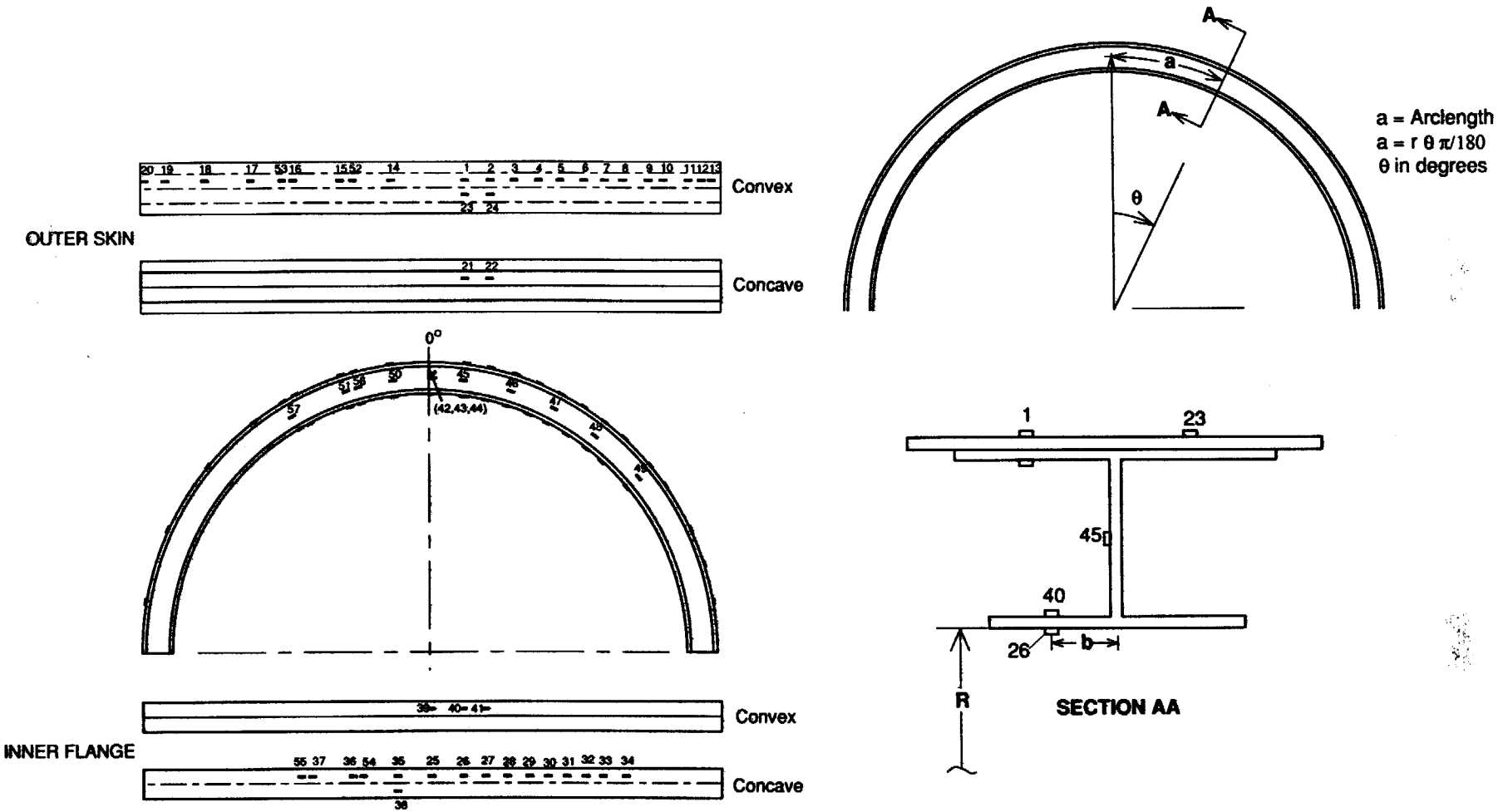

(a) Side view and inner and outer surfaces.

(b) Cross-sectional view

Figure 3.- Strain gage placement on I-frame.

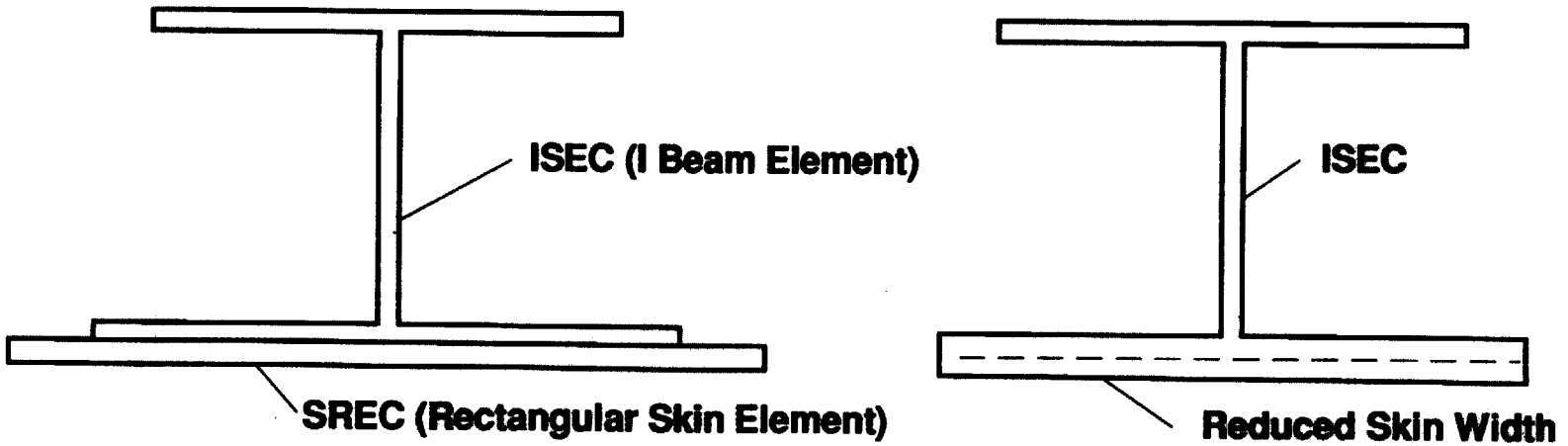

(a) Compound beam model

(b) Uniform I-beam model

Figure 4.- Cross-section of analytical models of composite I-frame.

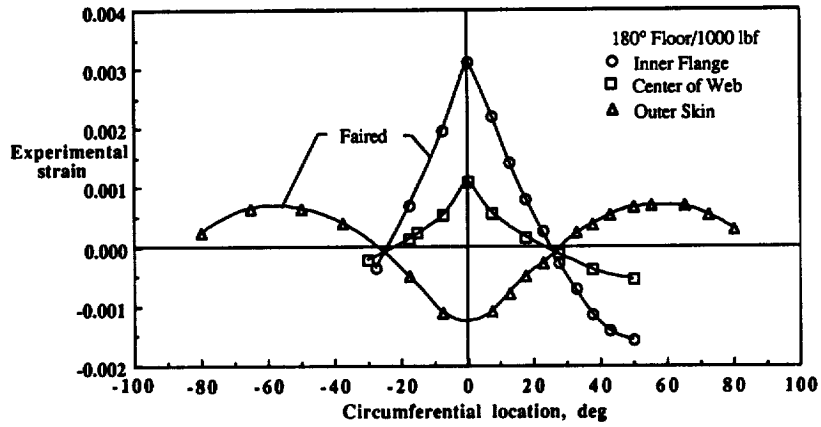

(a) 180° floor position.

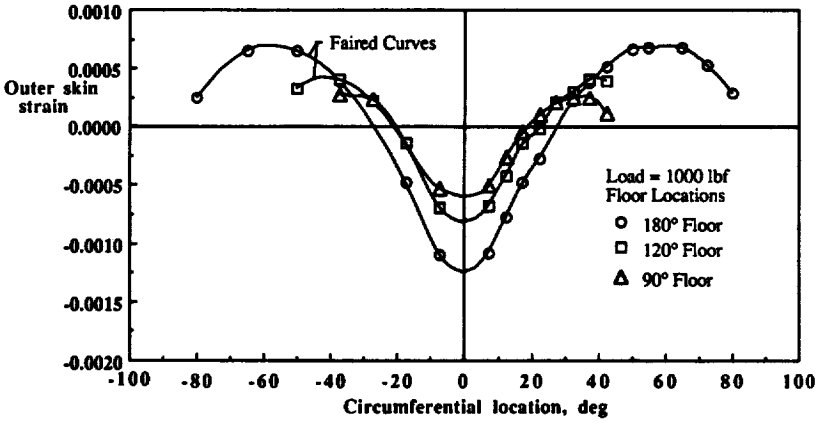

(b) 180°, 120°, and 90° floor positions.

Figure 5.- Typical experimental strain distributions on composite I-frame.

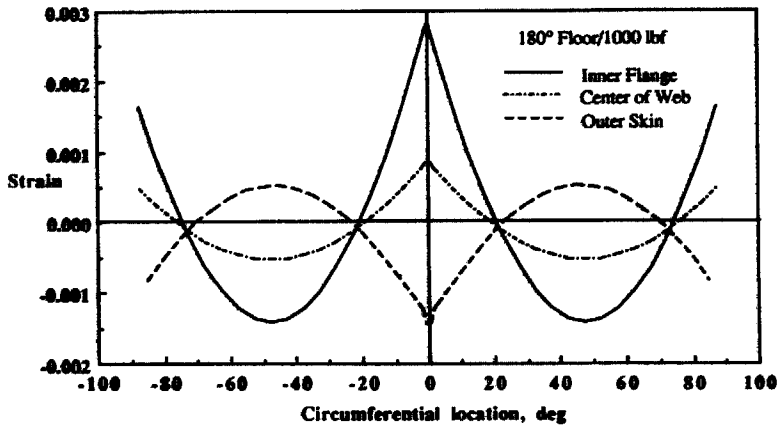

(a) Analytical 180° floor position.

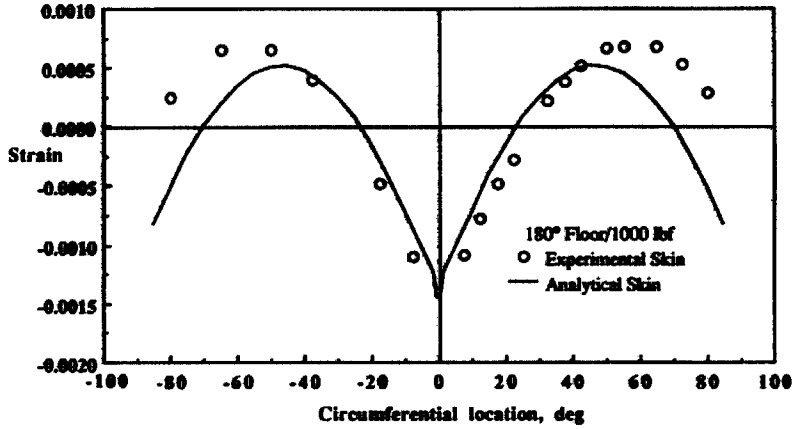

(b) Experimental and analytical comparison with original boundary condition.

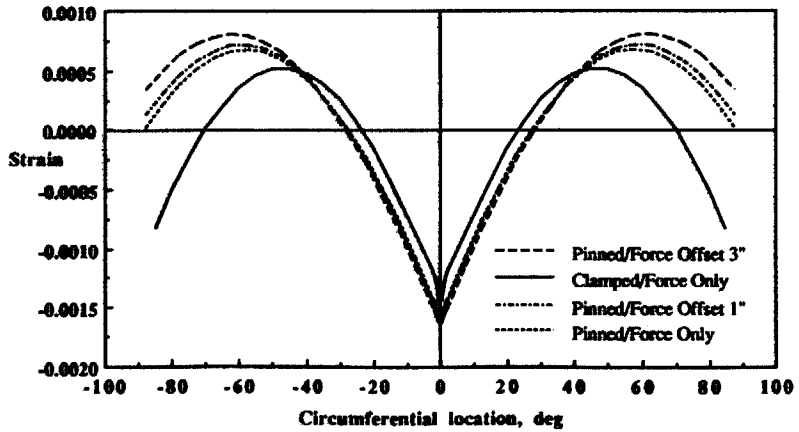

(c) Analytical boundary/loading results.

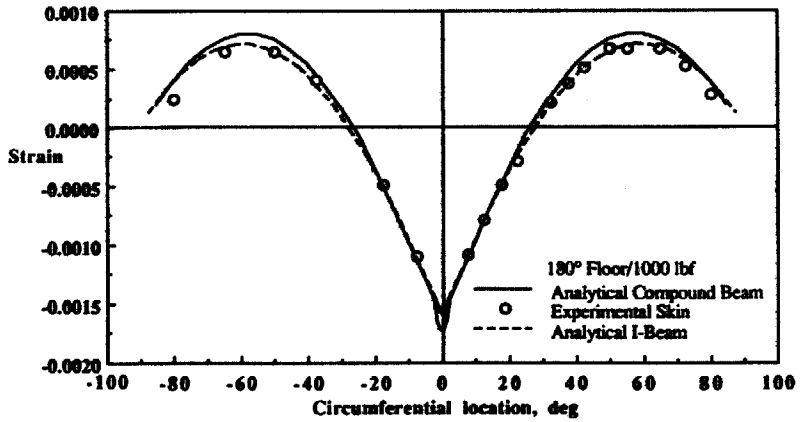

(d) Comparison of analytical models and experiment.

Figure 6.- Typical strain distribution on composite I-frame.

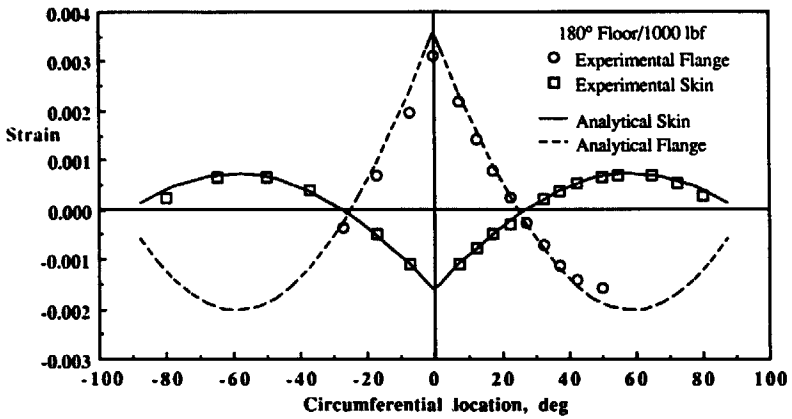

(a) Modified boundary and loading on 180° floor.

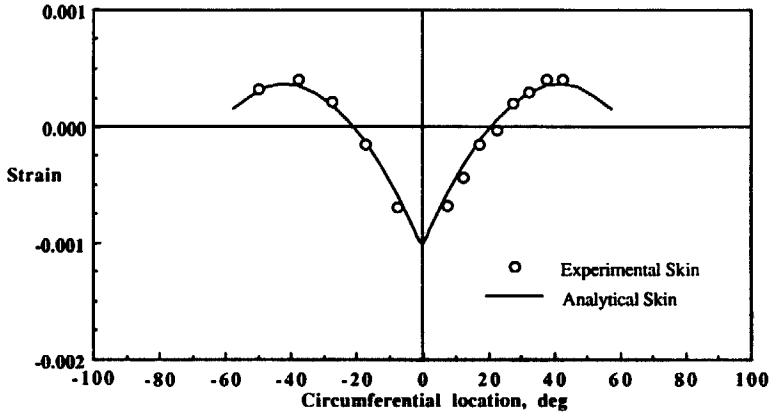

(b) Modified boundary and loading on 120° floor.

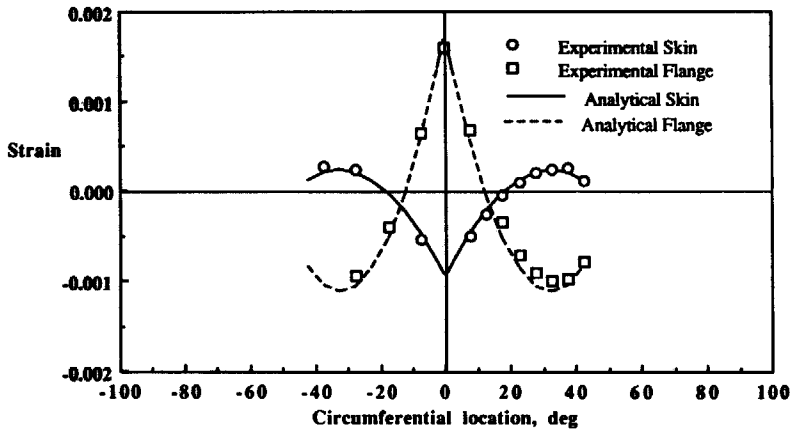

(c) Modified boundary and loading on 90° floor.

Figure 7.- Comparison of experimental and analytical strain distributions.

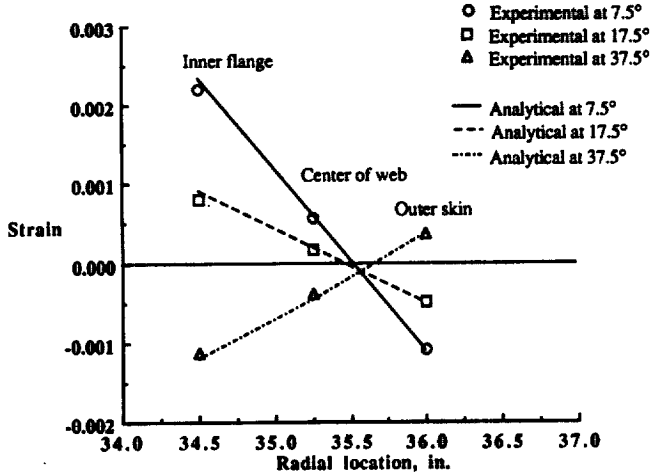

Figure 8.- Typical experimental and analytical radial strain distributions on I-frame with floor location at 180°.

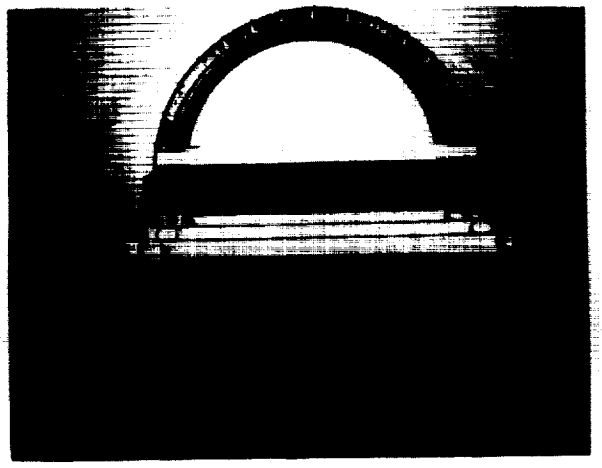

(a) Skinned and skeleton composite subfloors.

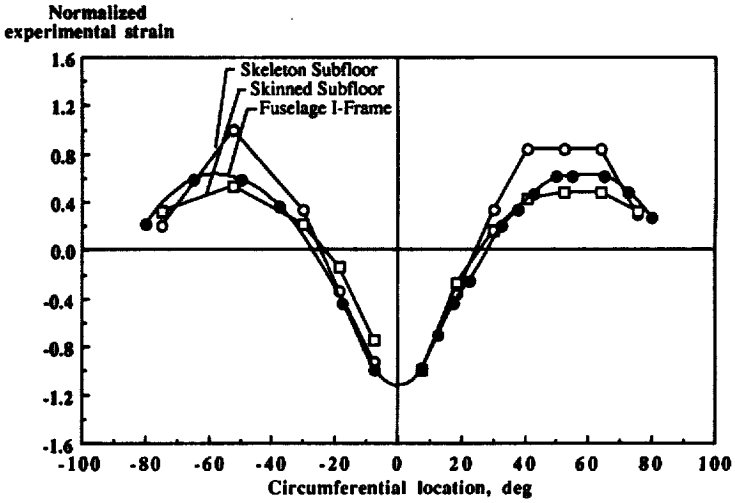

(b) Experimental normalized strain distributions.

Figure 9.- Typical composite structural specimens.

TABLE 1.-STRAIN GAGE LOCATIONS FOR COMPOSITE FRAME						
SG#	R, INCHES	THETA, DEG.	a, INCHES	b, INCHES	COMMENT	
1	36	7.5	4.71	(5/8)		
2	36	12.5	7.85	(5/8)		
3	36	17.5	11	(5/8)		
4	36	22.5	14.1	(5/8)		
5	36	27.5	17.3	(5/8)		
6	36	32.5	20.4	(5/8)		
7	36	37.5	23.6	(5/8)		
8	36	42.5	26.7	(5/8)		
9	36	50	31.4	(5/8)		
10	36	55	34.6	(5/8)		
11	36	65	40.8	(5/8)		
12	36	72.5	45.5	(5/8)		
13	36	80	50.3	(5/8)		
14	36	-7.5	-4.71	(5/8)		
15	36	-17.5	-11	(5/8)		
16	36	-27.5	-17.3	(5/8)		
17	36	-37.5	-23.6	(5/8)		
18	36	-50	-31.4	(5/8)		
19	36	-65	-40.8	(5/8)		
20	36	-80	-50.3	(5/8)		
21					BTB W/#1	
22					BTB W/#2	
23	36	7.5	4.71	-(5/8)		
24	36	12.5	7.85	-(5/8)		
25	36	0	0	(3/8)		
26	36	7.5	4.5	(3/8)		
27	34.5	12.5	7.5	(3/8)		
28	34.5	17.5	10.5	(3/8)		
29	34.5	22.5	13.5	(3/8)		
30	34.5	27.5	16.6	(3/8)		
31	34.5	32.5	19.6	(3/8)		
32	34.5	37.5	22.6	(3/8)		
33	34.5	42.5	25.6	(3/8)		
34	34.5	50	30.1	(3/8)		
35	34.5	-7.5	-4.5	(3/8)		
36	34.5	-17.5	-10.5	(3/8)		
37	34.5	-27.5	-16.6	(3/8)		
38	34.5	-7.5	-4.5	-(3/8)		
39					BTB W/#25	
40					BTB W/#26	
41					BTB W/#27	
42,43,44	35.25	0	0	0	ROSET/CLWEB	
45	35.25	7.5	4.6	0		
46	35.25	17.5	10.8	0		
47	35.25	27.5	16.9	0		
48	35.25	37.5	23.1	0		
49	35.25	50	30.8	0		
50	35.25	-7.5	-4.6	0		
51	35.25	-17.5	-10.8	0		
52	36	-15	-9.42	(5/8)		
53	36	-30	-18.85	(5/8)		
54	34.5	-15	-9.03	(3/8)		
55	34.5	-30	-18.06	(3/8)		
56	35.25	-15	-9.23	0		
57	35.25	-30	-18.46	0		

THIS PAGE INTENTIONALLY BLANK

omit

SESSION IV

DESIGN CRITERIA, RELIABILITY, SUPPORTABILITY

THIS PAGE INTENTIONALLY BLANK

omit

A Critical Review of Evolving Qualification Approaches for Contemporary Composite Airframes

Keith R. Kedward
University of California

John C. Halpin
Wright Aeronautical Systems Division

John E. McCarty
Consultant

THIS PAGE INTENTIONALLY BLANK